



Article

Calcium Regulation on the Atrial Regional Difference of Collagen Production Activity in Atrial Fibrogenesis

Cheng-Chih Chung^{1,2,3} , Yung-Kuo Lin^{1,2,3}, Yao-Chang Chen⁴, Yu-Hsun Kao^{5,6,*}, Yung-Hsin Yeh^{7,8} and Yi-Jen Chen^{1,2,3,5,*}

¹ Division of Cardiology, Department of Internal Medicine, School of Medicine, College of Medicine, Taipei Medical University, Taipei 11031, Taiwan; michaelchung110@gmail.com (C.-C.C.); yklin213@yahoo.com.tw (Y.-K.L.)

² Division of Cardiovascular Medicine, Department of Internal Medicine, Wan Fang Hospital, Taipei Medical University, Taipei 11696, Taiwan

³ Taipei Heart Institute, Taipei Medical University, Taipei 11031, Taiwan

⁴ Department of Biomedical Engineering, National Defense Medical Center, Taipei 11490, Taiwan; yaochang.chen@gmail.com

⁵ Graduate Institute of Clinical Medicine, College of Medicine, Taipei Medical University, Taipei 11031, Taiwan

⁶ Department of Medical Education and Research, Wan Fang Hospital, Taipei Medical University, Taipei 11696, Taiwan

⁷ Division of Cardiology, Chang Gung Memorial Hospital, Taoyuan 33305, Taiwan; yeongshinn@cgmh.org.tw

⁸ College of Medicine, Chang Gung University, Taoyuan 33302, Taiwan

* Correspondence: yuhsunkao@gmail.com (Y.-H.K.); yjchen@tmu.edu.tw (Y.-J.C.)



Citation: Chung, C.-C.; Lin, Y.-K.; Chen, Y.-C.; Kao, Y.-H.; Yeh, Y.-H.; Chen, Y.-J. Calcium Regulation on the Atrial Regional Difference of Collagen Production Activity in Atrial Fibrogenesis. *Biomedicines* **2021**, *9*, 686. <https://doi.org/10.3390/biomedicines9060686>

Academic Editor: Michal Tomcik

Received: 7 May 2021

Accepted: 15 June 2021

Published: 17 June 2021

Publisher's Note: MDPI stays neutral with regard to jurisdictional claims in published maps and institutional affiliations.



Copyright: © 2021 by the authors. Licensee MDPI, Basel, Switzerland. This article is an open access article distributed under the terms and conditions of the Creative Commons Attribution (CC BY) license (<https://creativecommons.org/licenses/by/4.0/>).

Abstract: Background: Atrial fibrosis plays an important role in the genesis of heart failure and atrial fibrillation. The left atrium (LA) exhibits a higher level of fibrosis than the right atrium (RA) in heart failure and atrial arrhythmia. However, the mechanism for the high fibrogenic potential of the LA fibroblasts remains unclear. Calcium (Ca^{2+}) signaling contributes to the pro-fibrotic activities of fibroblasts. This study investigated whether differences in Ca^{2+} homeostasis contribute to differential fibrogenesis in LA and RA fibroblasts. Methods: Ca^{2+} imaging, a patch clamp assay and Western blotting were performed in isolated rat LA and RA fibroblasts. Results: The LA fibroblasts exhibited a higher Ca^{2+} entry and gadolinium-sensitive current compared with the RA fibroblasts. The LA fibroblasts exhibited greater pro-collagen type I, type III, phosphorylated Ca^{2+} /calmodulin-dependent protein kinase II (CaMKII), phosphorylated phospholipase C (PLC), stromal interaction molecule 1 (STIM1) and transient receptor potential canonical (TRPC) 3 protein expression compared with RA fibroblasts. In the presence of 1 mmol/L ethylene glycol tetra-acetic acid (EGTA, Ca^{2+} chelator), the LA fibroblasts had similar pro-collagen type I, type III and phosphorylated CaMKII expression compared with RA fibroblasts. Moreover, in the presence of KN93 (a CaMKII inhibitor, 10 $\mu\text{mol/L}$), the LA fibroblasts had similar pro-collagen type I and type III compared with RA fibroblasts. Conclusion: The discrepancy of phosphorylated PLC signaling and gadolinium-sensitive Ca^{2+} channels in LA and RA fibroblasts induces different levels of Ca^{2+} influx, phosphorylated CaMKII expression and collagen production.

Keywords: fibroblasts; heart failure; left atrium; right atrium; Ca^{2+} ; CaMKII

1. Introduction

Atrial fibrosis contributes to the genesis of atrial arrhythmia and is the main manifestation of most cardiovascular diseases [1]. A higher level of atrial fibrosis was reported in patients with atrial myopathy or atrial arrhythmia or heart failure (HF) [1,2]. Left atrium (LA) fibrosis is a predictor in patients with atrial fibrillation (AF) [3]. The treatment of atrial fibrosis has been proven to decrease new-onset AF [4]. The LA and right atrium (RA) develop from different embryonic origins and exhibit dissimilar patterns of gene expression with different histological and immunohistochemical properties, which provide

multiple clues and targets for disease management [5,6]. The LA exhibits more advanced fibrosis than the RA in patients with atrial arrhythmia [7]. Compared with the RA, the LA exhibited a higher level of pro-fibrotic transcription factors and metalloproteinases in response to angiotensin II treatment [8–10]. The gene expression of *Smad 6*, which is an inhibitory messenger of pro-fibrotic cytokine signaling, is more highly expressed in RA than in LA tissues [11,12]. Our previous study revealed a higher collagen production in isolated rat LA fibroblasts than in their RA counterparts. Moreover, the LA had a higher level of fibrosis than the RA in rats with HF [13]. However, the underlying mechanism of the diverse response to pro-fibrotic signaling between LA and RA fibroblasts has not been fully elucidated.

Calcium (Ca^{2+}) signaling has been demonstrated to be downstream of multiple pro-fibrotic cytokines [14,15]. Human LA tissue exhibits higher *Pitx2c* expression as compared with RA tissue [16]. *Pitx2c* knockdown induces higher Ca^{2+} influx and fibroblast activity in human atrial fibroblasts [17]. Soluble guanylyl cyclase, a messenger that can decrease collagen production and Ca^{2+} entry, is highly expressed in RA tissues but markedly reduced or absent in LA tissues [18–20]. Compared with RA fibroblasts, LA fibroblasts produce a higher level of oxidative stress, which has been found to induce Ca^{2+} entry [13,21]. Increased intracellular Ca^{2+} is mainly derived either from extracellular Ca^{2+} entry or from endoplasmic reticulum (ER) Ca^{2+} release. Extracellular Ca^{2+} can enter cells through (1) voltage-operated Ca^{2+} channels, (2) transient receptor potential (TRP) channels and (3) Orai channels. Patients with AF had a higher expression of TRP channels. In addition, pro-fibrotic cytokines exert their pro-fibrotic effects on atrial fibroblasts through the activation of the TRP channels [22]. TRP canonical (TRPC) 3 and TRPC6 channel-induced Ca^{2+} influx makes a significant contribution to the pathogenesis of fibrosis [23,24]. TRPC3 and TRPC6 are mainly activated by phosphorylated phospholipase C (PLC)-induced diacylglycerol (DAG) [25,26]. PLC also activates inositol trisphosphate (IP3) signaling, inducing Ca^{2+} release from the endoplasmic reticulum (ER) [27,28].

The emptying of Ca^{2+} from the ER can be sensed by a stromal interaction molecule (STIM), a single-pass membrane protein in the ER membrane, thereby activating the store-operated Ca^{2+} entry [29]. Two kinds of STIM (STIM1, STIM2) were discovered in 2000–2001 [30,31]. Sensitized STIM1 clusters transform their conformation and are dominantly conjugated with the surface Orai protein, thereby inducing Ca^{2+} release-activated Ca^{2+} currents [32]. STIM1 has been found to play an important role in cardiac fibrogenesis [33]. STIM2 shares a 61% homology with STIM1 but exhibits different affinities with Ca^{2+} compared with STIM1 and acts as a regulator of the basal intracellular Ca^{2+} level [32,34,35]. The role of STIM2 on cardiac fibrogenesis has not been fully elucidated. However, the diversity of Ca^{2+} entry and the function and expression levels of these Ca^{2+} channels and the regulatory protein between LA and RA fibroblasts have not been fully elucidated. Increasing the Ca^{2+} influx enhances the collagen production capability of fibroblasts [36]. The purpose of the current study was to clarify whether Ca^{2+} signaling contributes to the differences in the collagen production capability between LA and RA fibroblasts.

In the present study, we investigated the Ca^{2+} influx and the membrane Ca^{2+} currents of LA and RA fibroblasts. We evaluated the role of extracellular Ca^{2+} influx and the downstream messenger on the diversity of pro-fibrotic cellular activities and compared the expressions of Ca^{2+} channels and regulatory proteins between LA and RA fibroblasts.

2. Materials and Methods

2.1. Isolation of LA and RA Cardiac Fibroblasts from Healthy Rats

The study was approved on 8 May 2018 by Laboratory Animal Committee of Taipei Medical University (approval number: LAC-2017-0383). LA and RA cardiac fibroblasts were isolated from male Sprague–Dawley (SD) rats (weighing 300–350 g) by using a modified protocol [13]. Briefly, after the animals were euthanized, the hearts were rapidly mounted on a Langendorff apparatus and perfused with phosphate-buffered saline containing 25 U/mL type 2 collagenase (Sigma, St. Louis, MO, USA) at 37 °C for 35 min.

LA and RA tissues were chopped and shaken in phosphate-buffered saline until single fibroblasts were obtained. The cells were filtered through a 40 μm cell strainer and then centrifuged at $300\times g$ for 10 min. Isolated atrial fibroblasts were cultured in 6 cm dishes in Dulbecco's modified Eagle's medium (Gibco, Paisley, UK) supplemented with 10% fetal bovine serum (Hyclone, Logan, UT, USA) and 100 U/mL penicillin-streptomycin (Gibco). After removing the pre-seeding medium containing the cardiomyocytes, the cells were incubated at 37 °C in the presence of 5% CO₂ for 48 h and were designated as passage 0 (P0) atrial fibroblasts. The cells were grown to confluence and sub-cultured to passage 1 (P1). P0 and P1 cells were positive for vimentin but negative for CD31 under immunofluorescence microscopy. α -smooth muscle actin was expressed in P1 cells but less in P0 cells (Supplementary Figure S1). P1 atrial fibroblasts, seeded at a density of 3×10^5 cells/cm² on culture dishes, were used in subsequent experiments and incubated in a serum-free medium for 24 h before each assay. P1 cells were used for Western blotting as more cells were required for the experiments.

2.2. Intracellular Ca²⁺ Imaging

Ca²⁺ imaging was performed as described previously [37]. The P0 atrial fibroblasts on 3 cm glass-bottom chamber slides were loaded with fura-2-acetoxymethyl ester (5 $\mu\text{mol/L}$; Invitrogen, Carlsbad, CA, USA) and Pluronic F-127 (20% solution in DMSO, 2.5 $\mu\text{g/mL}$) in a Ca²⁺-free solution containing (in mmol/L) NaCl 120, KCl 5.4, KH₂PO₄ 1.2, MgSO₄ 1.2, glucose 10, HEPES 6 and Taurine 8 (pH 7.40) for 30 min at 36 °C in a humidified incubator with 5% CO₂. Fura-2 fluorescence images were acquired using a Polychrome V (Till Photonics, Munich, Germany) monochromator mounted on an upright Leica DMI 3000B microscope with dual excitation wavelengths of 340 and 380 nm and an emission wavelength of 510 nm. The fura-2 images were analyzed using MetaFluor software version 7.7.6.0 (Molecular Devices, Sunnyvale, CA, USA). The ratio of F₃₄₀ to F₃₈₀ was used as a marker for the relative level of intracellular Ca²⁺. To measure Ca²⁺ entry, the cells were first exposed to the Ca²⁺-free solution for 8 min. The extracellular Ca²⁺ concentration was then increased to 10 mmol/L to measure Ca²⁺ entry through the store-operated channels activated by the Ca²⁺-store depletion. The intracellular Ca²⁺ was measured from the average of F₃₄₀/F₃₈₀ during 300–400 s under an extracellular-free Ca²⁺ solution (F₃₄₀/F₃₈₀-free Ca²⁺). The final peak of intracellular Ca²⁺ was measured from the average of F₃₄₀/F₃₈₀ during 2300–2400 s under 10 mmol/L Ca²⁺ solution (F₃₄₀/F₃₈₀ 10 mmol/L Ca²⁺). The change ($\Delta F_{340}/F_{380}$) between (F₃₄₀/F₃₈₀-free Ca²⁺) and (F₃₄₀/F₃₈₀ 10 mmol/L Ca²⁺) was used to represent the Ca²⁺ entry of each cell.

2.3. Patch Clamp Experiments

Subsequent to a gigaseal (seal resistance between 1–4 G Ω), a whole-cell patch clamp was performed on detached single P0 fibroblasts using an Axopatch 1D amplifier (Axon Instruments, Foster City, CA, USA) as described previously [24]. The area under the capacitive current was activated using a small hyperpolarizing step from a holding potential of -50 mV to a test potential of -55 mV for 80 milliseconds. The measured membrane resistance for P0 atrial fibroblasts was 0.49 ± 0.05 G Ω . When measuring gadolinium-sensitive currents, the detached fibroblasts were superfused with a Tyrode solution containing (mmol/L): NaCl 140, TEA-Cl 5.4, MgCl 1.0, CaCl₂ 2.0, glucose 10 and HEPES 10 with pH: 7.4 adjusted using CsOH. The pipette solution contained (mmol/L): CsCl₂ 135, CaCl₂ 0.1, EGTA 10, Mg-ATP 4.0, MgCl₂ 1.0, HEPES 10, Na-GTP 0.3, Na₂-phosphocreatine 6.6 with pH: 7.4 adjusted with CsOH. The currents were the differences before and after gadolinium (100 $\mu\text{mol/L}$, Sigma-Aldrich, St. Louis, MO, USA) recorded by a voltage ramps for 3 s ranging from -110 mV to $+100$ mV (0.07 mV/ms, 0.1 Hz) at 37 °C. Nifedipine (5 $\mu\text{mol/L}$) was used in the external solution to block any L-type Ca²⁺ current.

2.4. Western Blotting

Western blotting was performed as described previously [13]. In brief, P1 LA and RA fibroblasts treated with or without ethylene glycol tetra-acetic acid (EGTA, 1 mmol/L, Sigma-Aldrich) or a Ca^{2+} /calmodulin-dependent protein kinase II (CaMKII) inhibitor (KN93, 10 $\mu\text{mol/L}$, Sigma-Aldrich) were lysed in a radioimmunoprecipitation assay buffer containing 150 mmol/L NaCl, 0.5% sodium deoxycholate, 1% NP40, 50 mmol/L Tris pH 7.4, 0.1% sodium dodecyl sulfate (SDS) and protease inhibitor cocktails (Sigma). The proteins were fractionated using 10% SDS-polyacrylamide gel electrophoresis and transferred onto an equilibrated polyvinylidene difluoride membrane (Amersham Biosciences, Buckinghamshire, UK). The membranes were then incubated with primary antibodies against pro-collagen type III (1:3000, monoclonal, clone number: FH-7A, Abcam, Cambridge, UK); pro-collagen type IA1 (1:500, monoclonal, clone number: 3G3, Santa-Cruz Biotechnology, Santa Cruz, CA, USA); PLC- γ 1 (1:500, polyclonal, Cell Signaling Technology, Beverly, MA, USA); STIM1 (1:2000, monoclonal, clone number: 44, BD Transduction Laboratories, San Diego, CA, USA); phosphorylated CaMKII (1:3000, polyclonal, Abcam); Orai (1:2000, polyclonal, PROSCI, Poway, CA, USA); TRPC3 (1:1000, polyclonal, Abcam); and TRPC6 (1:3000, polyclonal, Alomone Labs, Jerusalem, Israel) and secondary antibodies. The bound antibodies were visualized using an ECL detection system (Millipore, Darmstadt, Germany) and analyzed with AlphaEaseFC software version 4.0.0 (Alpha Innotech, San Leandro, CA, USA). GAPDH (Sigma) was used as the loading control and normalized to the value of LA control fibroblasts.

2.5. Induction of Heart Failure

The induction of heart failure was performed as described previously [13]. Whole HF was induced in male Sprague–Dawley rats (weighing 300–350 g) by a subcutaneous injection of a high dose of isoproterenol (100 mg/kg). HF rats were euthanized 12 days after the isoproterenol injection for HF LA and RA fibroblast isolation.

2.6. Statistical Analysis

All quantitative data are expressed as a mean \pm standard error of the mean. The differences between LA and RA cardiac fibroblasts were compared using the unpaired *t*-test, paired *t*-test, Mann–Whitney rank-sum test or Wilcoxon signed-rank test depending on the outcome of the normality test. The differences between the different groups were compared by a two-way repeated ANOVA test with a post hoc of a Fisher LSD test. A *p* value of <0.05 was considered statistically significant.

3. Results

3.1. Diversity in Ca^{2+} Entry Between Isolated P0 LA and RA Fibroblasts from Healthy Rats

To evaluate the Ca^{2+} entry diversity between LA and RA P0 fibroblasts, these cells were first incubated with a Ca^{2+} -free extracellular solution to deplete the Ca^{2+} stores. Ca^{2+} entry was induced after increasing extracellular Ca^{2+} to 10 mmol/L. A fura-2 fluorescence image revealed that P0 LA fibroblasts exhibited a higher Ca^{2+} entry compared with P0 RA fibroblasts in healthy rats (Figure 1). Gadolinium has been considered as a non-specific TRP channel inhibitor [24]. We evaluated a gadolinium-sensitive cation current in the patch clamp experiments to study the role of the TRP channels in the diversity of Ca^{2+} entry between LA and RA fibroblasts. We found that P0 LA fibroblasts from healthy rats showed higher gadolinium-sensitive currents compared with P0 RA fibroblasts (Figure 2).

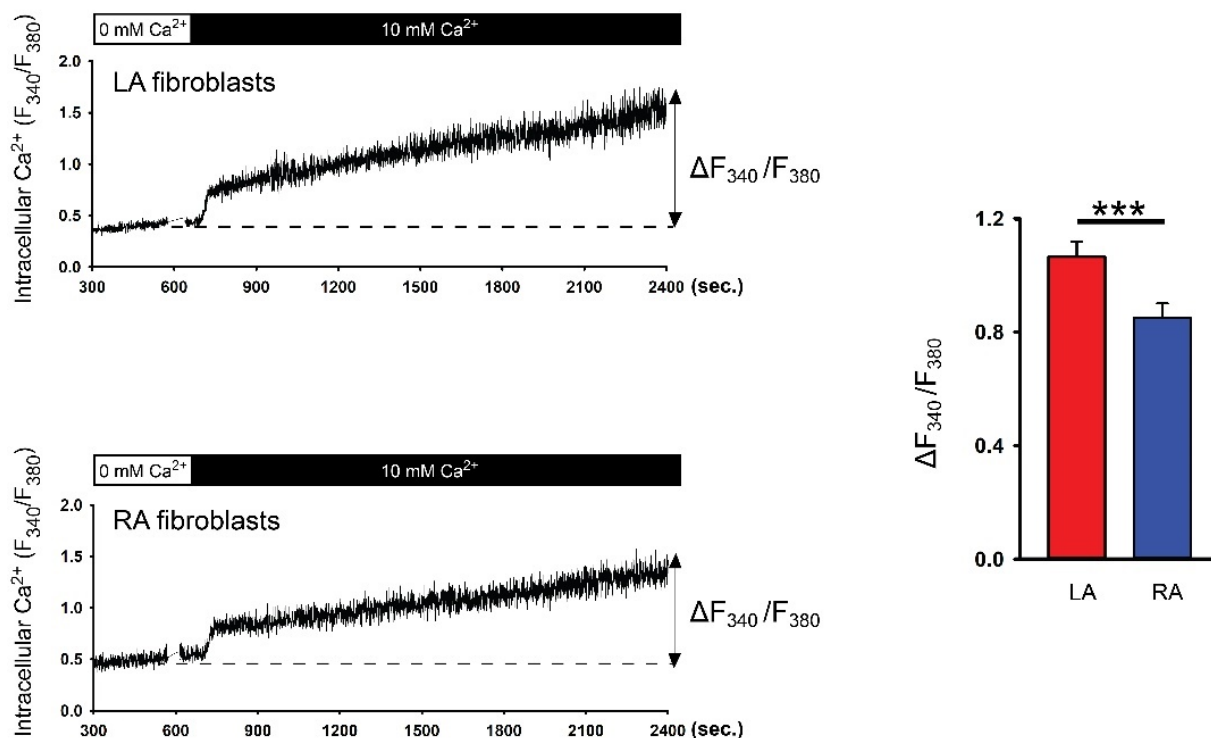


Figure 1. Ca²⁺ entry in the isolated passage 0 (P0) left atrium (LA) and right atrium (RA) fibroblasts from healthy rats. Left panels represent intracellular Ca²⁺ tracing from the LA fibroblasts (upper tracing, n = 18 LA fibroblasts from four rats) and RA fibroblasts (lower tracing, n = 17 RA fibroblasts from four rats). The cells were first incubated with a Ca²⁺-free extracellular solution to deplete the Ca²⁺ stores. Ca²⁺ entry was induced after increasing extracellular Ca²⁺ to 10 mmol/L. Right panels show the change in intracellular Ca²⁺ from a Ca²⁺-free solution to a 10 mmol/L Ca²⁺ solution ($\Delta F_{340}/F_{380}$). *** $p < 0.005$.

3.2. Differences in Ca²⁺ Signaling between Cultured P1 LA and RA Fibroblasts from Healthy Rats

LA fibroblasts exhibited higher pro-collagen type I, type III and phosphorylated CaMKII expressions compared with RA fibroblasts. EGTA is an extracellular Ca²⁺ chelator and has been used to evaluate the role of extracellular Ca²⁺ on Ca²⁺ entry in various cellular activities [38]. In the present study, EGTA (1 mmol/L) treatment reduced pro-collagen type I, type III and phosphorylated CaMKII expressions in LA fibroblasts. EGTA treatment reduced phosphorylated CaMKII but not the pro-collagen type I and type III expressions in RA fibroblasts. Furthermore, in the presence of EGTA (1 mmol/L), LA and RA fibroblasts had similar pro-collagen type I, type III and phosphorylated CaMKII expressions suggesting that differential pro-fibrotic activity between the primary isolated LA and RA fibroblasts was endogenously regulated by Ca²⁺ entry (Figure 3). We studied the molecular expression of PLC in LA and RA fibroblasts and found that LA fibroblasts had a greater phosphorylated PLC level (Figure 4). Moreover, LA fibroblasts also showed a greater STIM1 expression suggesting that LA fibroblasts may have upregulated the store-operated Ca²⁺ entry compared with RA fibroblasts (Figure 4). To evaluate the downstream signaling of PLC, we studied the expression levels of TRPC3 and TRPC6 and found that LA fibroblasts expressed a higher TRPC3 compared with RA fibroblasts. However, LA and RA fibroblasts exhibited similar levels of Orai and TRPC6 expressions (Figure 4).

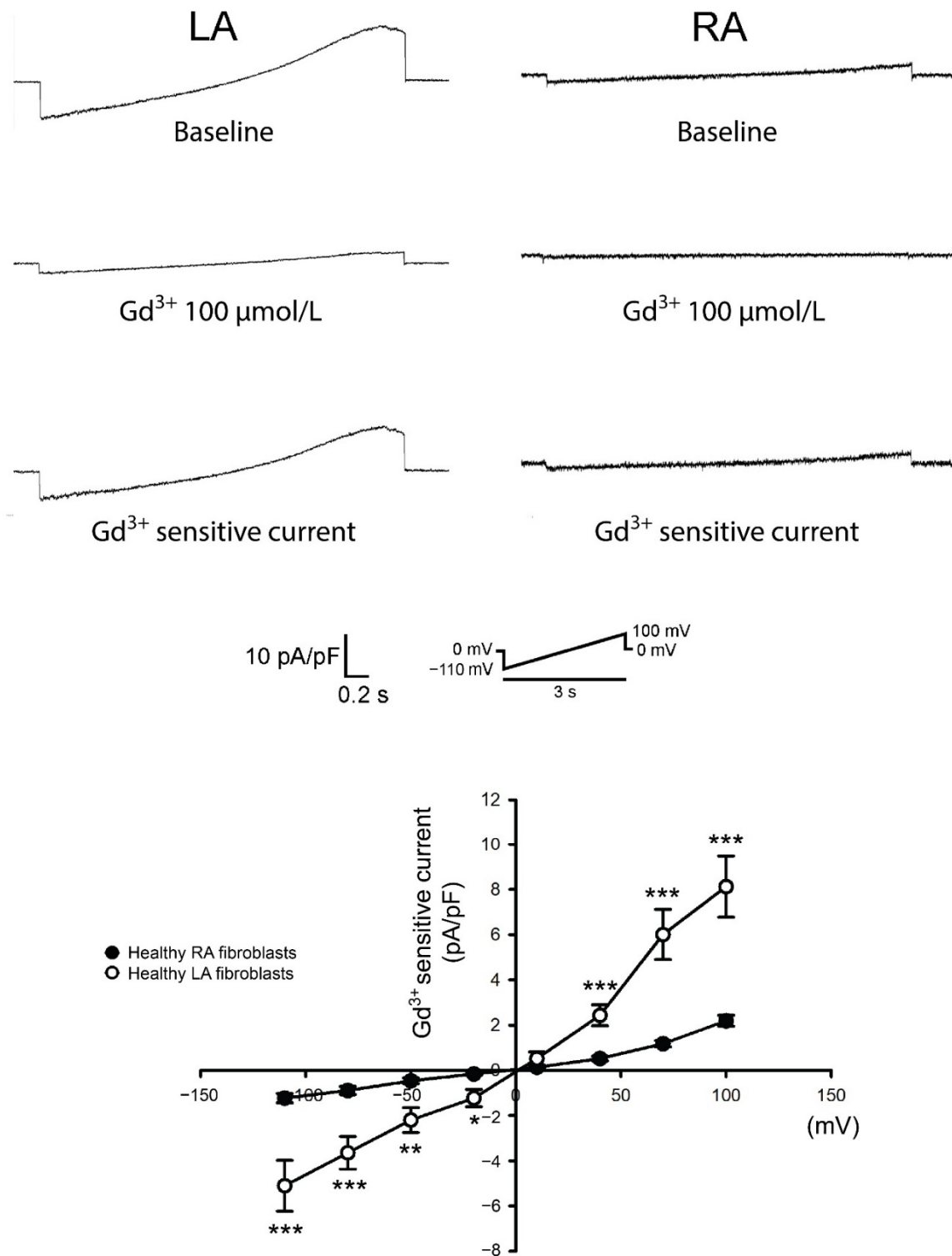


Figure 2. Membrane gadolinium (Gd³⁺)-sensitive currents in isolated passage 0 (P0) left atrium (LA) and right atrium (RA) fibroblasts from healthy rats. Left panels reveal tracings of the Gd³⁺ (100 μmol/L)-sensitive non-selective cation current from LA fibroblasts (n = 10 from five rats) and RA fibroblasts (n = 10 from five rats). Right panels reveal the current/voltage (I/V) relationship of the Gd³⁺-sensitive non-selective cation current. * *p* < 0.05, ** *p* < 0.01, *** *p* < 0.005. The insets in the current traces show the various clamp protocols.

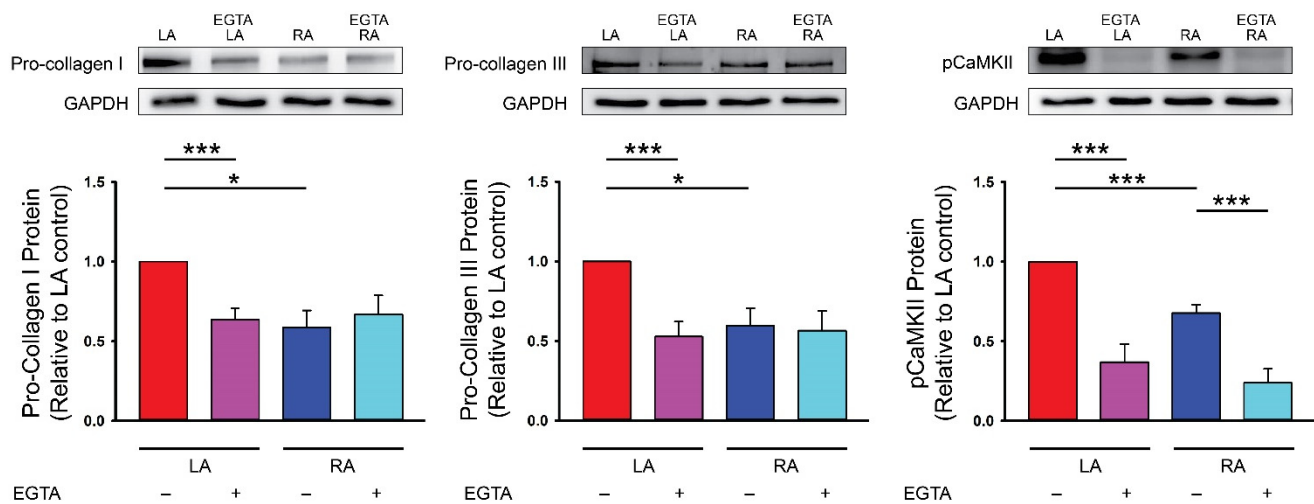


Figure 3. Ca^{2+} entry on the diversity of the collagen production ability in the cultured passage 1 (P1) left atrium (LA) and right atrium (RA) fibroblasts from healthy rats. Photographs and averaged data of the pro-collagen type I (n = 6 independent experiments), pro-collagen type III (n = 6 independent experiments) and phosphorylated Ca^{2+} /calmodulin-dependent protein kinase II (pCaMKII, n = 6 independent experiments) expression in LA and RA fibroblasts with or without 1 mmol/L ethylene glycol tetra-acetic acid (EGTA, an extracellular Ca^{2+} chelator) for 48 h. GAPDH was used as a loading control. * $p < 0.05$, *** $p < 0.005$.

We used KN93 (10 $\mu\text{mol/L}$, a CaMKII inhibitor) to evaluate the role of higher phosphorylated CaMKII in the LA fibroblasts and found that the LA and RA fibroblasts exhibited similar pro-collagen type I and type III levels in the presence of KN93 (Figure 4) suggesting that CaMKII phosphorylation regulated the diversity of the collagen production between LA and RA fibroblasts.

3.3. Differences in Gadolinium-Sensitive Currents between Isolated P0 LA and RA Fibroblasts from HF Rats

In our previous study [13], we found that in HF rats, LA tissues expressed higher fibrotic levels compared with RA tissues. We evaluated the diversity of Ca^{2+} homeostasis between HF LA and HF RA fibroblasts. We found that P0 LA fibroblasts from HF rats showed higher gadolinium-sensitive currents compared with P0 RA fibroblasts (Figure 5). Moreover, compared to healthy P0 LA fibroblasts, HF P0 LA fibroblasts exhibited higher gadolinium-sensitive currents (Supplementary Figure S2), which was comparable with the findings of previous studies that HF fibroblasts exhibited upregulated currents through TRP channels compared with fibroblasts from healthy subjects [24,39]. However, HF RA and healthy RA fibroblasts had similar gadolinium-sensitive currents.

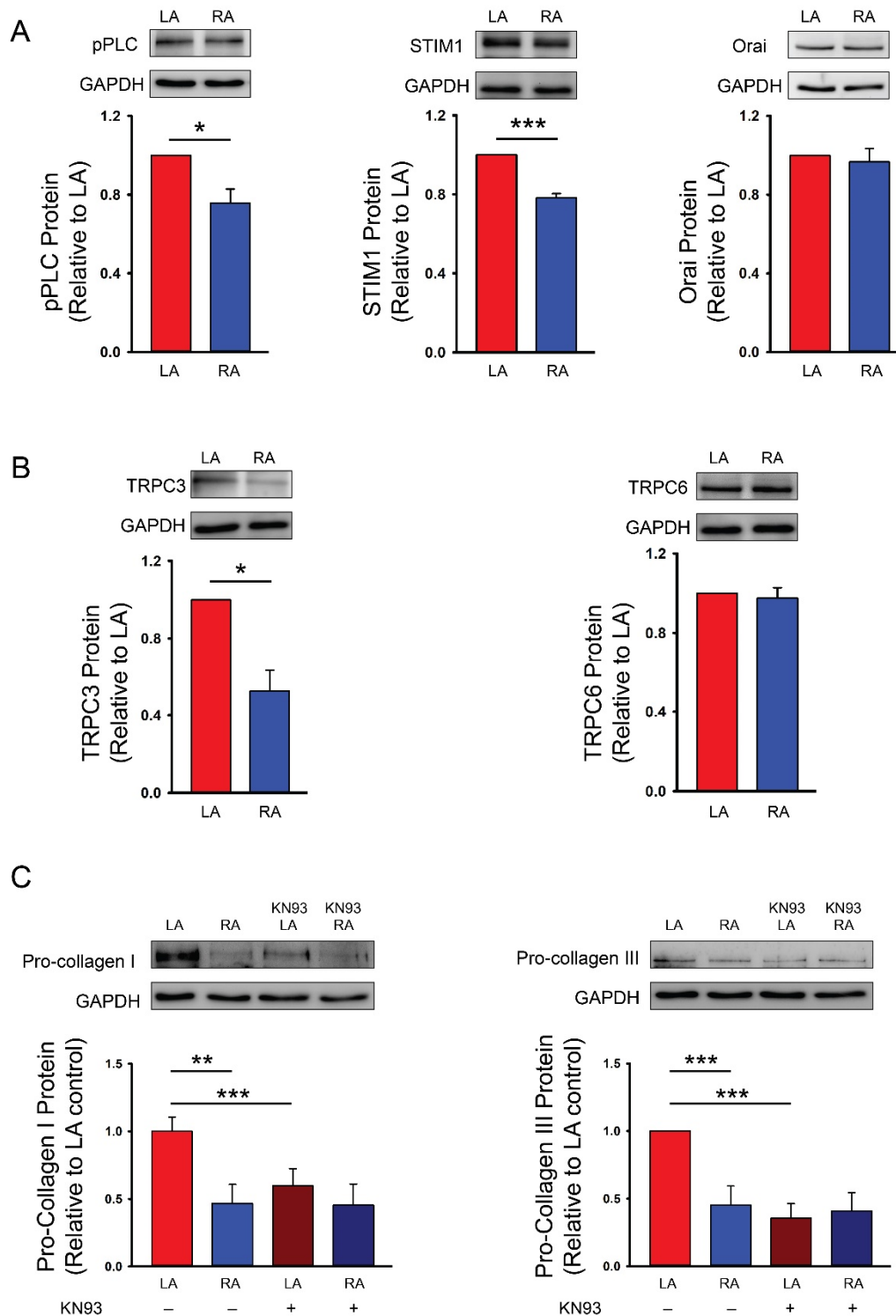


Figure 4. Ca^{2+} signaling pathway on the diversity of the collagen production capability between the cultured passage 1 (P1) left atrial (LA) and right atrial (RA) fibroblasts from healthy rats. (A) Photographs and averaged data of the phosphorylated phospholipase C (pPLC, $n = 5$ independent experiments), stromal interaction molecule 1 (STIM1, $n = 5$ independent experiments) and Orai ($n = 5$ independent experiments) expression of LA and RA fibroblasts. (B) Photographs and averaged data of the transient receptor potential canonical (TRPC) 3 (TRPC3, $n = 5$ independent experiments) and TRPC6 ($n = 5$ independent experiments) expression of LA and RA fibroblasts. (C) Photographs and averaged data of the pro-collagen type I ($n = 5$ independent experiments) and pro-collagen type III ($n = 5$ independent experiments) expression of LA and RA fibroblasts with or without a Ca^{2+} /calmodulin-dependent protein kinase II (CaMKII) inhibitor (KN93, 10 $\mu\text{mol/L}$) for 48 h. GAPDH was used as a loading control. * $p < 0.05$, ** $p < 0.01$, *** $p < 0.005$.

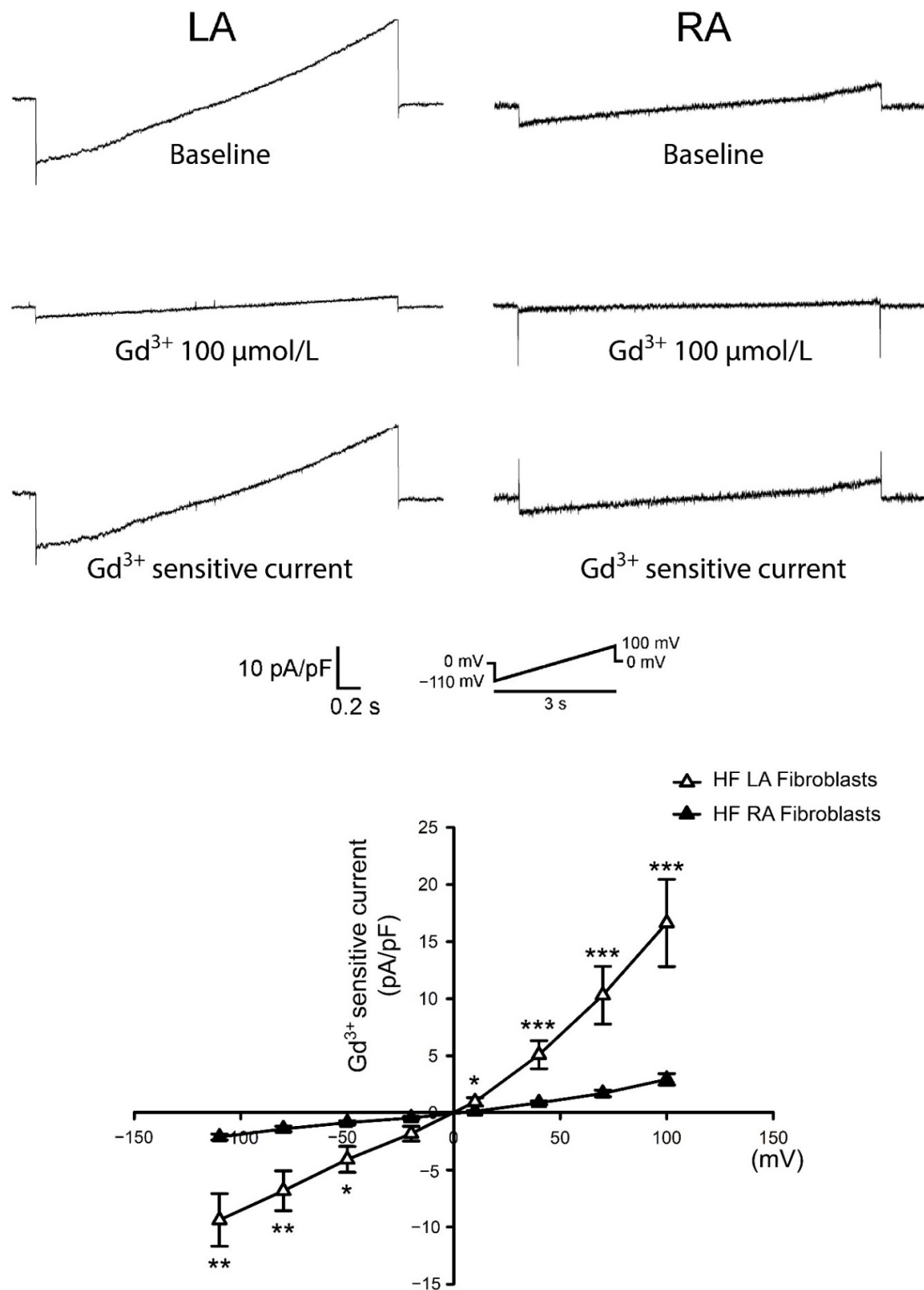


Figure 5. Membrane gadolinium (Gd³⁺)-sensitive currents in isolated passage 0 (P0) left atrium (LA) and right atrium (RA) fibroblasts from heart failure (HF) rats. Left panels reveal tracings of the Gd³⁺ (100 μmol/L)-sensitive non-selective cation current from HF LA fibroblasts (n = 10 from six rats), HF RA fibroblasts (n = 10 from five rats). Right panels reveal the current/voltage (I/V) relationship of the Gd³⁺-sensitive non-selective cation current. * *p* < 0.05, ** *p* < 0.01, *** *p* < 0.005. The insets in the current traces show the various clamp protocols.

4. Discussion

A higher degree of fibrosis in the LA than the RA has been found in various cardiovascular diseases [13,40]. The Ca^{2+} signaling pathway plays an important role in pro-fibrotic cellular activities. However, whether Ca^{2+} homeostasis contributes to the diversity between LA and RA fibroblasts remains unclear. Here we have shown, for the first time, that a difference in the Ca^{2+} signaling induced the collagen production between LA and RA fibroblasts. We found that the Ca^{2+} entry capability was greater in isolated rat LA fibroblasts than in their RA counterparts from healthy rats. In addition, EGTA-treated LA and RA fibroblasts exhibited a similar collagen production ability, indicating that the Ca^{2+} influx activated the augmented pro-fibrotic activities in LA fibroblasts. Ca^{2+} influx has been the target of treatment for various fibrotic diseases. Fibroblasts isolated from patients with systemic sclerosis exerted their activated pro-fibrotic cellular activities through a Ca^{2+} influx [41]. Transforming growth factor (TGF)- β augmented collagen production through promoting Ca^{2+} entry whereas EGTA attenuated TGF- β -mediated collagen production in renal fibroblasts [42]. A platelet-derived growth factor (PDGF) evoked a Ca^{2+} influx thereby inducing the collagen production of lung fibroblasts [15]. Compared with RA tissue, LA tissue exhibited higher levels of calcitonin gene-related peptide, which is a cardiovascular neurotransmitter that can increase the intracellular Ca^{2+} amount through Ca^{2+} entry [43,44]. In addition, a pro-fibrotic protease chymase, which is highly expressed in LA tissues but not in RA tissues, can induce Ca^{2+} entry [45–47]. Accordingly, LA fibroblasts may constitutionally exhibit a higher Ca^{2+} influx capability compared with RA fibroblasts.

Pro-fibrotic cytokines such as TGF- β or PDGF induce an extracellular matrix production through the PLC signaling pathway [15,48]. The inhibition of phospholipase C signaling can decrease the collagen production capabilities of lung fibroblasts [49]. Studies have evaluated the differences between the LA and the RA. A genomic study revealed that the gene expression in LA tissue had a greater involvement in Wnt signaling compared with RA tissue in patients with AF [50]. The non-canonical Wnt signaling pathway activates phosphorylated PLC, thereby increasing IP3 production and inducing Ca^{2+} homeostasis [51]. The gene expression of aldose reductase, which is a protein that can activate the PLC signaling pathway and enhance Ca^{2+} influx, is more highly expressed in LA than in RA tissues [11,52,53]. Moreover, the activation of the Notch signaling pathway was found in the LA but not in the RA in patients with atrial arrhythmia [54]. Notch activation can upregulate STIM1 expression and activate store-operated Ca^{2+} entry [55,56]. The present study showed that LA fibroblasts expressed a higher level of phosphorylated PLC and STIM1 compared with RA fibroblasts. Our findings suggested a high propensity for Ca^{2+} homeostasis in LA fibroblasts, which might contribute to a higher fibrogenesis in LA fibroblasts compared with their RA counterparts. The expression of the STIM1/Orai conjugation was positively correlated with a greater collagen production capability in cardiac fibroblasts [57]. The different levels of STIM1 in LA and RA fibroblasts may also contribute to the diversity of collagen production via the activation of the Orai channel. However, as we studied atrial fibrogenesis using healthy cells taken from healthy tissues it is not clear whether these findings can be translated to pathological conditions.

We found that the gadolinium-sensitive current was higher in LA fibroblasts than RA fibroblasts isolated from healthy rats. Compared with RA fibroblasts, LA fibroblasts exhibited higher expression levels of TRPC3 but not TRPC6. Genetically knocking out TRPC3 attenuated myocardial fibrosis in pressure-overloaded HF mice [58]. Our findings suggested that the higher gadolinium-sensitive current in LA fibroblasts might be related to the TRPC3 channel. The diversities in the electrophysiologic characteristics between LA and RA tissues have been studied [59]. LA tissues exhibited a higher inward-rectifier potassium channel gene expression compared with RA tissues [60]. Differences in electrophysiologic currents have been found between the LA and left ventricular fibroblasts [61]. Moreover, we found that in rats with HF, isolated LA fibroblasts also exhibited higher gadolinium-sensitive currents compared with isolated RA fibroblasts. Accordingly, we may speculate that, compared with RA fibroblasts, LA fibroblasts exhibited more currents through TRPC3,

thereby exhibiting a greater collagen production capability. However, gadolinium has been proven to inhibit currents through Orai channels [62,63]. Gadolinium-sensitive currents could also be the result of STIM-Orai-dependent store-operated calcium entry.

CaMKII, triggered by Ca^{2+} /calmodulin-induced auto-phosphorylation, is a downstream messenger of the Ca^{2+} signaling pathway [64]. CaMKII activation contributes to pathological cardiac remodeling as the expression is upregulated in patients with AF or HF [65,66]. CaMKII activation augments the collagen production in cardiac fibroblasts [67]. Moreover, genetically knocking-down CaMKII or a treatment with KN93 was shown to reduce myocardial fibrosis in mice with pathological remodeling [68,69]. KN93 can also inhibit the proliferation, collagen production and pro-fibrotic cytokine production capability of cardiac fibroblasts [67]. Our study showed that EGTA-treated LA and RA fibroblasts had similar levels of phosphorylated CaMKII. LA and RA fibroblasts had a similar collagen production capability upon KN93 treatment suggesting that a higher Ca^{2+} influx induced the CaMKII signaling pathway further, thereby activating the augmented pro-fibrotic cellular activity of LA fibroblasts. Figure 6 shows the proposed mechanism that contributed to the differential collagen production in LA and RA fibroblasts. The diversities of phosphorylated PLC signaling and the expression of TRPC3 and STIM1 activated different levels of Ca^{2+} influx resulting in a different phosphorylated CaMKII expression and collagen production between LA and RA fibroblasts.

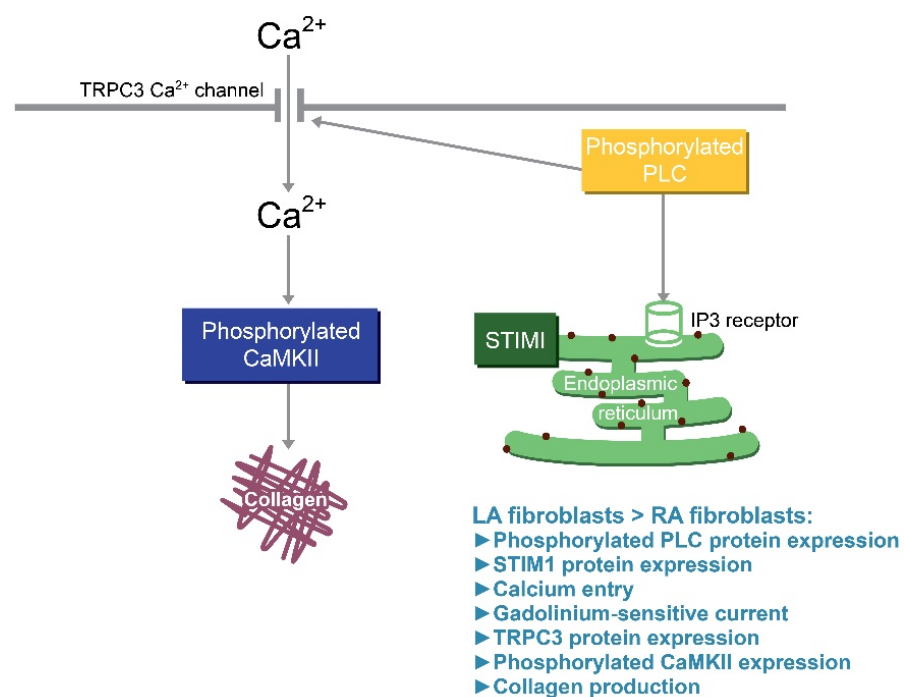


Figure 6. Illustration of the proposed mechanism that contributes to the differential collagen production in left atrium (LA) and right atrium (RA) fibroblasts. The diversities of the phosphorylated phospholipase C (pPLC) signaling and the expression of transient receptor potential canonical (TRPC) 3 Ca^{2+} channels activate different levels of Ca^{2+} influx, which may induce a different phosphorylated Ca^{2+} /calmodulin-dependent protein kinase II (CaMKII) expression and collagen production between LA and RA fibroblasts. The different levels of stromal interaction molecule 1 (STIM1) in LA and RA fibroblasts may also contribute to the diversity of collagen production via the activation of the Orai channel. IP3: Inositol trisphosphate.

There were a few limitations in this study. Although gadolinium has been used as a non-specific TRP channel blocker for years [70,71], gadolinium can also indirectly inhibit ATP-gated P2X receptor cation (P2X) or chloride channels [72,73]. Hence, it is not clear whether P2X or chloride channels contributed to the diversity of the Ca^{2+} influx [74,75]. In

In addition, this study found a different constitutive discrepancy in the Ca^{2+} currents between LA and RA fibroblasts but the displayed currents were unspecific due to no activation stimulus (receptor stimulation, direct agonists, etc.) being applied. Moreover, the cells were incubated in a nominal calcium-free solution [24], which might be insufficient to induce a proper calcium store depletion. The addition of EGTA to the extracellular solution and the inhibition of the SERCA pumps with cyclopiazonic acid or thapsigargin is regularly used to empty calcium stores. However, this study did not use this method to avoid ER stress-induced fibroblast death [76] as the cells were primarily isolated and invulnerable to this treatment. Therefore, our findings might underestimate the differences of LA and RA fibroblasts on ER Ca^{2+} release. Finally, part of the diversity of the Ca^{2+} level at the end of Ca^{2+} imaging might be also due to the differences in the cytosolic calcium clearance between LA and RA fibroblasts as our study did not clarify the role of the SERCA pump and plasma membrane Ca^{2+} ATPase (PMCA) pump in the Ca^{2+} imaging.

In conclusion, the discrepancy of phosphorylated PLC signaling and gadolinium-sensitive Ca^{2+} channels in LA and RA fibroblasts induced different levels of Ca^{2+} influx, phosphorylated CaMKII expression and collagen production.

Supplementary Materials: The following are available online at <https://www.mdpi.com/article/10.3390/biomedicines9060686/s1>, Figure S1: α -smooth muscle actin (α -SMA) expression in passage 0 (P0) and passage 1 (P1) left atrium (LA) and right atrium (RA) fibroblasts. Figure S2: Current/voltage (I/V) relationship of the membrane gadolinium (Gd^{3+})-sensitive currents in isolated passage 0 (P0) left atrium (LA) and right atrium (RA) fibroblasts from healthy and heart failure (HF) rats.

Author Contributions: Conceptualization, C.-C.C., Y.-H.K. and Y.-J.C.; formal analysis, C.-C.C., Y.-K.L. and Y.-C.C.; investigation, C.-C.C., Y.-K.L. and Y.-C.C.; resources, C.-C.C. and Y.-H.Y.; data curation, C.-C.C., Y.-K.L., Y.-C.C., Y.-H.Y., Y.-H.K. and Y.-J.C.; writing—original draft preparation, C.-C.C.; writing—review and editing, Y.-H.K., Y.-H.Y. and Y.-J.C.; supervision, Y.-H.K. and Y.-J.C. All authors have read and agreed to the published version of the manuscript.

Funding: This work was supported by the Taipei Medical University-Wan Fang Hospital (107-wf-swf-07) and the Ministry of Science and Technology of Taiwan (MOST 108-2314-B-038-117-MY3).

Institutional Review Board Statement: All animal studies were performed according to the protocols approved on 8th, May, 2018 by the Laboratory Animal Committee of Taipei Medical University (Approval number: LAC-2017-0383).

Data Availability Statement: The data that support the findings of this study are available from the corresponding author upon reasonable request.

Acknowledgments: The authors acknowledge the technical services of calcium image experiments provided by the Instrument Center of National Defense Medical Center. The authors acknowledge the Laboratory Animal Center at TMU for technical support in the fibroblast isolation experiment.

Conflicts of Interest: The authors declare no conflict of interest.

References

1. Kostin, S.; Klein, G.; Szalay, Z.; Hein, S.; Bauer, E.P.; Schaper, J. Structural correlate of atrial fibrillation in human patients. *Cardiovasc. Res.* **2002**, *54*, 361–379. [[CrossRef](#)]
2. Ohtani, K.; Yutani, C.; Nagata, S.; Koretsune, Y.; Hori, M.; Kamada, T. High prevalence of atrial fibrosis in patients with dilated cardiomyopathy. *J. Am. Coll. Cardiol.* **1995**, *25*, 1162–1169. [[CrossRef](#)]
3. Azadani, P.N.; King, J.B.; Kheirikhahan, M.; Chang, L.; Marrouche, N.F.; Wilson, B.D. Left atrial fibrosis is associated with new-onset heart failure in patients with atrial fibrillation. *Int. J. Cardiol.* **2017**, *248*, 161–165. [[CrossRef](#)] [[PubMed](#)]
4. Swedberg, K.; Zannad, F.; McMurray, J.J.V.; Krum, H.; van Veldhuisen, D.J.; Shi, H.; Vincent, J.; Pitt, B. Eplerenone and atrial fibrillation in mild systolic heart failure: Results from the EMPHASIS-HF (Eplerenone in Mild Patients Hospitalization And Survival Study in Heart Failure) study. *J. Am. Coll. Cardiol.* **2012**, *59*, 1598–1603. [[CrossRef](#)] [[PubMed](#)]
5. Tabibiazar, R.; Wagner, R.A.; Liao, A.; Quertermous, T. Transcriptional profiling of the heart reveals chamber-specific gene expression patterns. *Circ. Res.* **2003**, *93*, 1193–1201. [[CrossRef](#)] [[PubMed](#)]
6. Kahr, P.C.; Piccini, I.; Fabritz, L.; Greber, B.; Schöler, H.; Scheld, H.H.; Hoffmeier, A.; Brown, N.A.; Kirchhof, P. Systematic analysis of gene expression differences between left and right atria in different mouse strains and in human atrial tissue. *PLoS ONE* **2011**, *6*, e26389. [[CrossRef](#)] [[PubMed](#)]

7. Park, J.H.; Lee, J.S.; Ko, Y.G.; Lee, S.H.; Lee, B.S.; Kang, S.M.; Chang, B.C.; Pak, H.N. Histological and biochemical comparisons between right atrium and left atrium in patients with mitral valvular atrial fibrillation. *Korean Circ. J.* **2014**, *44*, 233–242. [[CrossRef](#)] [[PubMed](#)]
8. Hasin, T.; Elhanani, O.; Abassi, Z.; Hai, T.; Aronheim, A. Angiotensin II signaling up-regulates the immediate early transcription factor ATF3 in the left but not the right atrium. *Basic Res. Cardiol.* **2011**, *106*, 175–187. [[CrossRef](#)] [[PubMed](#)]
9. Koren, L.; Elhanani, O.; Kehat, I.; Hai, T.; Aronheim, A. Adult cardiac expression of the activating transcription factor 3, ATF3, promotes ventricular hypertrophy. *PLoS ONE* **2013**, *8*, e68396. [[CrossRef](#)]
10. Jansen, H.J.; Mackasey, M.; Moghtadaei, M.; Belke, D.D.; Egom, E.E.; Tuomi, J.M.; Rafferty, S.A.; Kirkby, A.W.; Rose, R.A. Distinct patterns of atrial electrical and structural remodeling in angiotensin II mediated atrial fibrillation. *J. Mol. Cell. Cardiol.* **2018**, *124*, 12–25. [[CrossRef](#)]
11. Lin, H.; Dolmatova, E.V.; Morley, M.P.; Lunetta, K.L.; McManus, D.D.; Magnani, J.W.; Margulies, K.B.; Hakonarson, H.; del Monte, F.; Benjamin, E.J.; et al. Gene expression and genetic variation in human atria. *Heart Rhythm* **2014**, *11*, 266–271. [[CrossRef](#)]
12. Seet, L.F.; Toh, L.Z.; Finger, S.N.; Chu, S.W.L.; Stefanovic, B.; Wong, T.T. Valproic acid suppresses collagen by selective regulation of Smads in conjunctival fibrosis. *J. Mol. Med. (Berlin)* **2016**, *94*, 321–334. [[CrossRef](#)]
13. Chung, C.C.; Kao, Y.H.; Yao, C.J.; Lin, Y.K.; Chen, Y.J. A comparison of left and right atrial fibroblasts reveals different collagen production activity and stress-induced mitogen-activated protein kinase signalling in rats. *Acta Physiol.* **2017**, *220*, 432–445. [[CrossRef](#)] [[PubMed](#)]
14. Mukherjee, S.; Kolb, M.R.J.; Duan, F.; Janssen, L.J. Transforming growth factor- β evokes Ca^{2+} waves and enhances gene expression in human pulmonary fibroblasts. *Am. J. Respir. Cell Mol. Biol.* **2012**, *46*, 757–764. [[CrossRef](#)]
15. Mukherjee, S.; Duan, F.; Kolb, M.R.J.; Janssen, L.J. Platelet derived growth factor-evoked Ca^{2+} wave and matrix gene expression through phospholipase C in human pulmonary fibroblast. *Int. J. Biochem. Cell Biol.* **2013**, *45*, 1516–1524. [[CrossRef](#)] [[PubMed](#)]
16. Kirchhof, P.; Kahr, P.C.; Kaese, S.; Piccini, I.; Vokshi, I.; Scheld, H.H.; Rotering, H.; Fortmueller, L.; Laakmann, S.; Verheule, S.; et al. *PITX2c* is expressed in the adult left atrium, and reducing *Pitx2c* expression promotes atrial fibrillation inducibility and complex changes in gene expression. *Circ. Cardiovasc. Genet.* **2011**, *4*, 123–133. [[CrossRef](#)] [[PubMed](#)]
17. Kao, Y.H.; Chung, C.C.; Cheng, W.L.; Lkhagva, B.; Chen, Y.J. *Pitx2c* inhibition increases atrial fibroblast activity: Implications in atrial arrhythmogenesis. *Eur. J. Clin. Investig.* **2019**, *49*, e13160. [[CrossRef](#)]
18. Mookerjee, I.; Hewitson, T.D.; Halls, M.L.; Summers, R.J.; Mathai, M.L.; Bathgate, R.A.D.; Tregear, G.W.; Samuel, C.S. Relaxin inhibits renal myofibroblast differentiation via *RXFPI*, the nitric oxide pathway, and Smad2. *FASEB J.* **2009**, *23*, 1219–1229. [[CrossRef](#)]
19. Mendes-Silverio, C.B.; Leiria, L.O.S.; Morganti, R.P.; Anhê, G.F.; Marcondes, S.; Mônica, F.Z.; De Nucci, G.; Antunes, E. Activation of haem-oxidized soluble guanylyl cyclase with BAY 60-2770 in human platelets lead to overstimulation of the cyclic GMP signaling pathway. *PLoS ONE* **2012**, *7*, e47223. [[CrossRef](#)]
20. Brahmajothi, M.V.; Campbell, D.L. Heterogeneous expression of NO-activated soluble guanylyl cyclase in mammalian heart: Implications for NO- and redox-mediated indirect versus direct regulation of cardiac ion channel function. *Channels (Austin Tex)* **2007**, *1*, 353–365. [[CrossRef](#)]
21. Oronowicz, J.; Reinhard, J.; Reinach, P.S.; Ludwiczak, S.; Luo, H.; Omar Ba Salem, M.H.; Kraemer, M.M.; Biebermann, H.; Kakkassery, V.; Mergler, S. Ascorbate-induced oxidative stress mediates TRP channel activation and cytotoxicity in human etoposide-sensitive and -resistant retinoblastoma cells. *Lab. Investig.* **2021**, *101*, 70–88. [[CrossRef](#)]
22. Du, J.; Xie, J.; Zhang, Z.; Tsujikawa, H.; Fusco, D.; Silverman, D.; Liang, B.; Yue, L. TRPM7-mediated Ca^{2+} signals confer fibrogenesis in human atrial fibrillation. *Circ. Res.* **2010**, *106*, 992–1003. [[CrossRef](#)]
23. Hofmann, K.; Fiedler, S.; Vierkotten, S.; Weber, J.; Klee, S.; Jia, J.; Zwickenpflug, W.; Flockerzi, V.; Storch, U.; Yildirim, A.Ö.; et al. Classical transient receptor potential 6 (TRPC6) channels support myofibroblast differentiation and development of experimental pulmonary fibrosis. *Biochim. Biophys. Acta Mol. Basis Dis.* **2017**, *1863*, 560–568. [[CrossRef](#)]
24. Harada, M.; Luo, X.; Qi, X.Y.; Tadevosyan, A.; Maguy, A.; Ordog, B.; Ledoux, J.; Kato, T.; Naud, P.; Voigt, N.; et al. Transient receptor potential canonical-3 channel-dependent fibroblast regulation in atrial fibrillation. *Circulation* **2012**, *126*, 2051–2064. [[CrossRef](#)] [[PubMed](#)]
25. Wedel, B.; Boyles, R.R.; Putney, J.W., Jr.; Bird, G.S. Role of the store-operated calcium entry proteins Stim1 and Orai1 in muscarinic cholinergic receptor-stimulated calcium oscillations in human embryonic kidney cells. *J. Physiol.* **2007**, *579*, 679–689. [[CrossRef](#)] [[PubMed](#)]
26. Hofmann, T.; Obukhov, A.G.; Schaefer, M.; Harteneck, C.; Gudermann, T.; Schultz, G. Direct activation of human TRPC6 and TRPC3 channels by diacylglycerol. *Nature* **1999**, *397*, 259–263. [[CrossRef](#)] [[PubMed](#)]
27. Essen, L.O.; Perisic, O.; Katan, M.; Wu, Y.; Roberts, M.F.; Williams, R.L. Structural mapping of the catalytic mechanism for a mammalian phosphoinositide-specific phospholipase C. *Biochemistry* **1997**, *36*, 1704–1718. [[CrossRef](#)] [[PubMed](#)]
28. Moccia, F.; Dragoni, S.; Lodola, F.; Bonetti, E.; Bottino, C.; Guerra, G.; Laforenza, U.; Rosti, V.; Tanzi, F. Store-dependent Ca^{2+} entry in endothelial progenitor cells as a perspective tool to enhance cell-based therapy and adverse tumour vascularization. *Curr. Med. Chem.* **2012**, *19*, 5802–5818. [[CrossRef](#)]
29. Stathopoulos, P.B.; Zheng, L.; Li, G.Y.; Plevin, M.J.; Ikura, M. Structural and mechanistic insights into STIM1-mediated initiation of store-operated calcium entry. *Cell* **2008**, *135*, 110–122. [[CrossRef](#)]
30. Manji, S.S.; Parker, N.J.; Williams, R.T.; van Stekelenburg, L.; Pearson, R.B.; Dziadek, M.; Smith, P.J. STIM1: A novel phosphoprotein located at the cell surface. *Biochim. Biophys. Acta* **2000**, *1481*, 147–155. [[CrossRef](#)]

31. Williams, R.T.; Manji, S.S.; Parker, N.J.; Hancock, M.S.; Van Stekelenburg, L.; Eid, J.P.; Senior, P.V.; Kazenwadel, J.S.; Shandala, T.; Saint, R.; et al. Identification and characterization of the STIM (stromal interaction molecule) gene family: Coding for a novel class of transmembrane proteins. *Biochem. J.* **2001**, *357*, 673–685. [[CrossRef](#)]
32. Muik, M.; Schindl, R.; Fahrner, M.; Romanin, C. Ca(2+) release-activated Ca(2+) (CRAC) current, structure, and function. *Cell Mol. Life Sci.* **2012**, *69*, 4163–4176. [[CrossRef](#)] [[PubMed](#)]
33. Zhang, B.; Jiang, J.; Yue, Z.; Liu, S.; Ma, Y.; Yu, N.; Gao, Y.; Sun, S.; Chen, S.; Liu, P. Store-Operated Ca²⁺ Entry (SOCE) contributes to angiotensin II-induced cardiac fibrosis in cardiac fibroblasts. *J. Pharmacol. Sci.* **2016**, *132*, 171–180. [[CrossRef](#)] [[PubMed](#)]
34. Stathopoulos, P.B.; Zheng, L.; Ikura, M. Stromal interaction molecule (STIM) 1 and STIM2 calcium sensing regions exhibit distinct unfolding and oligomerization kinetics. *J. Biol. Chem.* **2009**, *284*, 728–732. [[CrossRef](#)]
35. Brandman, O.; Liou, J.; Park, W.S.; Meyer, T. STIM2 is a feedback regulator that stabilizes basal cytosolic and endoplasmic reticulum Ca²⁺ levels. *Cell* **2007**, *131*, 1327–1339. [[CrossRef](#)]
36. Brilla, C.G.; Scheer, C.; Rupp, H. Angiotensin II and intracellular calcium of adult cardiac fibroblasts. *J. Mol. Cell Cardiol.* **1998**, *30*, 1237–1246. [[CrossRef](#)] [[PubMed](#)]
37. Chung, C.C.; Lin, Y.K.; Chen, Y.C.; Kao, Y.H.; Yeh, Y.H.; Chen, Y.J. Factor Xa inhibition by rivaroxaban regulates fibrogenesis in human atrial fibroblasts with modulation of nitric oxide synthesis and calcium homeostasis. *J. Mol. Cell Cardiol.* **2018**, *123*, 128–138. [[CrossRef](#)]
38. Ziemba, B.P.; Falke, J.J. A PKC-MARCKS-PI3K regulatory module links Ca²⁺ and PIP3 signals at the leading edge of polarized macrophages. *PLoS ONE* **2018**, *13*, e0196678. [[CrossRef](#)]
39. Feng, J.; Zong, P.; Yan, J.; Yue, Z.; Li, X.; Smith, C.; Ai, X.; Yue, L. Upregulation of transient receptor potential melastatin 4 (TRPM4) in ventricular fibroblasts from heart failure patients. *Pflugers Arch.* **2021**, *473*, 521–531. [[CrossRef](#)]
40. Akoum, N.; McGann, C.; Vergara, G.; Badger, T.; Ranjan, R.; Mahnkopf, C.; Kholmovski, E.; Macleod, R.O.B.; Marrouche, N. Atrial fibrosis quantified using late gadolinium enhancement MRI is associated with sinus node dysfunction requiring pacemaker implant. *J. Cardiovasc. Electrophysiol.* **2012**, *23*, 44–50. [[CrossRef](#)]
41. Wu, C.Y.; Hsu, W.L.; Tsai, M.H.; Chai, C.Y.; Yen, C.J.; Chen, C.H.; Lu, J.H.; Yu, H.S.; Yoshioka, T. A potential new approach for treating systemic sclerosis: Dedifferentiation of SSc fibroblasts and change in the microenvironment by blocking store-operated Ca²⁺ entry. *PLoS ONE* **2019**, *14*, e0213400. [[CrossRef](#)] [[PubMed](#)]
42. Gooch, J.L.; Gorin, Y.; Zhang, B.X.; Abboud, H.E. Involvement of calcineurin in transforming growth factor-beta-mediated regulation of extracellular matrix accumulation. *J. Biol. Chem.* **2004**, *279*, 15561–15570. [[CrossRef](#)]
43. Chang, Y.; Stover, S.R.; Hoover, D.B. Regional localization and abundance of calcitonin gene-related peptide receptors in guinea pig heart. *J. Mol. Cell Cardiol.* **2001**, *33*, 745–754. [[CrossRef](#)] [[PubMed](#)]
44. Al-Rubaiee, M.; Gangula, P.R.; Millis, R.M.; Walker, R.K.; Umoh, N.A.; Cousins, V.M.; Jeffress, M.A.; Haddad, G.E. Inotropic and lusitropic effects of calcitonin gene-related peptide in the heart. *Am. J. Physiol. Heart Circ. Physiol.* **2013**, *304*, H1525–H1537. [[CrossRef](#)] [[PubMed](#)]
45. Wang, H.; Varagic, J.; Nagata, S.; Kon, N.D.; Ahmad, S.; VonCannon, J.L.; Wright, K.N.; Sun, X.; Deal, D.; Groban, L.; et al. Differential expression of the angiotensin-(1-12)/chymase axis in human atrial tissue. *J. Surg. Res.* **2020**, *253*, 173–184. [[CrossRef](#)] [[PubMed](#)]
46. Lang, Y.D.; Chang, S.F.; Wang, L.F.; Chen, C.M. Chymase mediates paraquat-induced collagen production in human lung fibroblasts. *Toxicol. Lett.* **2010**, *193*, 19–25. [[CrossRef](#)]
47. Saito, K.; Muto, T.; Tomimori, Y.; Maruoka, H.; Tanaka, T.; Fukuda, Y. Human chymase stimulates Ca²⁺ signaling in human polymorphonuclear cells. *Immunol. Lett.* **2003**, *89*, 161–165. [[CrossRef](#)]
48. Kucich, U.; Rosenbloom, J.C.; Shen, G.; Abrams, W.R.; Hamilton, A.D.; Sebt, S.M.; Rosenbloom, J. TGF-beta1 stimulation of fibronectin transcription in cultured human lung fibroblasts requires active geranylgeranyl transferase I, phosphatidylcholine-specific phospholipase C, protein kinase C-delta, and p38, but not erk1/erk2. *Arch. Biochem. Biophys.* **2000**, *374*, 313–324. [[CrossRef](#)] [[PubMed](#)]
49. Vazquez-de-Lara, L.G.; Tlatelpa-Romero, B.; Romero, Y.; Fernández-Tamayo, N.; Vazquez-de-Lara, F.; Justo-Janeiro, J.M.; Garcia-Carrasco, M.; de-la-Rosa, P.R.; Cisneros-Lira, J.G.; Mendoza-Milla, C.; et al. Phosphatidylethanolamine Induces an Antifibrotic Phenotype in Normal Human Lung Fibroblasts and Ameliorates Bleomycin-Induced Lung Fibrosis in Mice. *Int. J. Mol. Sci.* **2018**, *19*, 2758. [[CrossRef](#)]
50. Thomas, A.M.; Cabrera, C.P.; Finlay, M.; Lall, K.; Nobles, M.; Schilling, R.J.; Wood, K.; Mein, C.A.; Barnes, M.R.; Munroe, P.B.; et al. Differentially expressed genes for atrial fibrillation identified by RNA sequencing from paired human left and right atrial appendages. *Physiol. Genomics* **2019**, *51*, 323–332. [[CrossRef](#)]
51. Zhang, J.; Chandrasekaran, G.; Li, W.; Kim, D.Y.; Jeong, I.Y.; Lee, S.H.; Liang, T.; Bae, J.Y.; Choi, I.; Kang, H.; et al. Wnt-PLC-IP 3-Connexin-Ca²⁺ axis maintains ependymal motile cilia in zebrafish spinal cord. *Nat. Commun.* **2020**, *11*, 1860. [[CrossRef](#)] [[PubMed](#)]
52. Pal, P.B.; Sonowal, H.; Shukla, K.; Srivastava, S.K.; Ramana, K.V. Aldose reductase mediates NLRP3 inflammasome-initiated innate immune response in hyperglycemia-induced Thp1 monocytes and male mice. *Endocrinology* **2017**, *158*, 3661–3675. [[CrossRef](#)] [[PubMed](#)]
53. Wang, C.; La, L.; Feng, H.; Yang, Q.; Wu, F.; Wang, C.; Wu, J.; Hou, L.; Hou, C.; Liu, W. Aldose reductase inhibitor engeletin suppresses pelvic inflammatory disease by blocking the phospholipase C/protein kinase C-dependent/NF-κB and MAPK cascades. *J. Agric. Food Chem.* **2020**, *68*, 11747–11757. [[CrossRef](#)]

54. Lipovsky, C.E.; Jimenez, J.; Guo, Q.; Li, G.; Yin, T.; Hicks, S.C.; Bhatnagar, S.; Takahashi, K.; Zhang, D.M.; Brumback, B.D.; et al. Chamber-specific transcriptional responses in atrial fibrillation. *JCI Insight* **2020**, *5*, e135319. [[CrossRef](#)]
55. Song, S.; Babicheva, A.; Zhao, T.; Ayon, R.J.; Rodriguez, M.; Rahimi, S.; Balistrieri, F.; Harrington, A.; Shyy, J.Y.J.; Thistlethwaite, P.A.; et al. Notch enhances Ca²⁺ entry by activating calcium-sensing receptors and inhibiting voltage-gated K⁺ channels. *Am. J. Physiol. Cell Physiol.* **2020**, *318*, C954–C968. [[CrossRef](#)] [[PubMed](#)]
56. Liu, X.; Wang, T.; Wang, Y.; Chen, Z.; Hua, D.; Yao, X.; Ma, X.; Zhang, P. Orai1 is critical for Notch-driven aggressiveness under hypoxic conditions in triple-negative breast cancers. *Biochim. Biophys. Acta Mol. Basis Dis.* **2018**, *1864*, 975–986. [[CrossRef](#)] [[PubMed](#)]
57. Ross, G.R.; Bajwa, T., Jr.; Edwards, S.; Emelyanova, L.; Rizvi, F.; Holmuhamedov, E.L.; Werner, P.; Downey, F.X.; Tajik, A.J.; Jahangir, A. Enhanced store-operated Ca²⁺ influx and Orai1 expression in ventricular fibroblasts from human failing heart. *Biol. Open* **2017**, *6*, 326–332.
58. Numaga-Tomita, T.; Kitajima, N.; Kuroda, T.; Nishimura, A.; Miyano, K.; Yasuda, S.; Kuwahara, K.; Sato, Y.; Ide, T.; Birnbaumer, L.; et al. TRPC3-GEF-H1 axis mediates pressure overload-induced cardiac fibrosis. *Sci. Rep.* **2016**, *6*, 39383. [[CrossRef](#)]
59. Tai, C.T.; Lo, L.W.; Lin, Y.J.; Chen, S.A. Arrhythmogenic difference between the left and right atria in a canine ventricular pacing-induced heart failure model of atrial fibrillation. *Pacing Clin. Electrophysiol.* **2012**, *35*, 188–195. [[CrossRef](#)]
60. Swartz, M.F.; Fink, G.W.; Lutz, C.J.; Taffet, S.M.; Berenfeld, O.; Vikstrom, K.L.; Kasprovicz, K.; Bhatta, L.; Puskas, F.; Kalifa, J.; et al. Left versus right atrial difference in dominant frequency, K(+) channel transcripts, and fibrosis in patients developing atrial fibrillation after cardiac surgery. *Heart Rhythm* **2009**, *6*, 1415–1422. [[CrossRef](#)]
61. Wu, C.T.; Qi, X.Y.; Huang, H.; Naud, P.; Dawson, K.; Yeh, Y.H.; Harada, M.; Kuo, C.T.; Nattel, S. Disease and region-related cardiac fibroblast potassium current variations and potential functional significance. *Cardiovasc. Res.* **2014**, *102*, 487–496. [[CrossRef](#)] [[PubMed](#)]
62. Giachini, F.R.C.; Chiao, C.W.; Carneiro, F.S.; Lima, V.V.; Carneiro, Z.N.; Dorrance, A.M.; Tostes, R.C.; Webb, R.C. Increased activation of stromal interaction molecule-1/Orai-1 in aorta from hypertensive rats: A novel insight into vascular dysfunction. *Hypertension* **2009**, *53*, 409–416. [[CrossRef](#)] [[PubMed](#)]
63. Chauvet, S.; Jarvis, L.; Chevallet, M.; Shrestha, N.; Groschner, K.; Bouron, A. Pharmacological characterization of the native store-operated calcium channels of cortical neurons from embryonic mouse brain. *Front. Pharmacol.* **2016**, *7*, 486. [[CrossRef](#)] [[PubMed](#)]
64. Means, A.R. Regulatory cascades involving calmodulin-dependent protein kinases. *Mol. Endocrinol.* **2000**, *14*, 4–13. [[CrossRef](#)] [[PubMed](#)]
65. Voigt, N.; Li, N.; Wang, Q.; Wang, W.; Trafford, A.W.; Abu-Taha, I.; Sun, Q.; Wieland, T.; Ravens, U.; Nattel, S.; et al. Enhanced sarcoplasmic reticulum Ca²⁺ leak and increased Na⁺-Ca²⁺ exchanger function underlie delayed afterdepolarizations in patients with chronic atrial fibrillation. *Circulation* **2012**, *125*, 2059–2070. [[CrossRef](#)]
66. Hoch, B.; Meyer, R.; Hetzer, R.; Krause, E.G.; Karczewski, P. Identification and expression of delta-isoforms of the multifunctional Ca²⁺/calmodulin-dependent protein kinase in failing and nonfailing human myocardium. *Circ. Res.* **1999**, *84*, 713–721. [[CrossRef](#)]
67. Zhang, W.; Chen, D.Q.; Qi, F.; Wang, J.; Xiao, W.Y.; Zhu, W.Z. Inhibition of calcium-calmodulin-dependent kinase II suppresses cardiac fibroblast proliferation and extracellular matrix secretion. *J. Cardiovasc. Pharmacol.* **2010**, *55*, 96–105. [[CrossRef](#)]
68. Kreusser, M.M.; Lehmann, L.H.; Wolf, N.; Keranov, S.; Jungmann, A.; Gröne, H.J.; Müller, O.J.; Katus, H.A.; Backs, J. Inducible cardiomyocyte-specific deletion of CaM kinase II protects from pressure overload-induced heart failure. *Basic Res. Cardiol.* **2016**, *111*, 65. [[CrossRef](#)]
69. Zhong, P.; Quan, D.; Peng, J.; Xiong, X.; Liu, Y.; Kong, B.; Huang, H. Role of CaMKII in free fatty acid/hyperlipidemia-induced cardiac remodeling both in vitro and in vivo. *J. Mol. Cell Cardiol.* **2017**, *109*, 1–16. [[CrossRef](#)]
70. Masuoka, T.; Yamashita, Y.; Yoshida, J.; Nakano, K.; Tawa, M.; Nishio, M.; Ishibashi, T. Sensitization of glutamate receptor-mediated pain behaviour via nerve growth factor-dependent phosphorylation of transient receptor potential V1 under inflammatory conditions. *Br. J. Pharmacol.* **2020**, *177*, 4223–4241. [[CrossRef](#)] [[PubMed](#)]
71. Siri-Angkul, N.; Song, Z.; Fefelova, N.; Gwathmey, J.K.; Chattipakorn, S.C.; Qu, Z.; Chattipakorn, N.; Xie, L.H. Activation of TRPC (transient receptor potential canonical) channel currents in iron overloaded cardiac myocytes. *Circ. Arrhythm Electrophysiol.* **2021**, *14*, e009291. [[CrossRef](#)] [[PubMed](#)]
72. Germinario, E.; Esposito, A.; Midrio, M.; Peron, S.; Palade, P.T.; Betto, R.; Danieli-Betto, D. High-frequency fatigue of skeletal muscle: Role of extracellular Ca(2+). *Eur. J. Appl. Physiol.* **2008**, *104*, 445–453. [[CrossRef](#)] [[PubMed](#)]
73. Nejime, N.; Kagota, S.; Tada, Y.; Nakamura, K.; Hashimoto, M.; Kunitomo, M.; Shinozuka, K. Possible participation of chloride ion channels in ATP release from cancer cells in suspension. *Clin. Exp. Pharmacol. Physiol.* **2009**, *36*, 278–282. [[CrossRef](#)]
74. Chen, J.B.; Tao, R.; Sun, H.Y.; Tse, H.F.; Lau, C.P.; Li, G.R. Multiple Ca²⁺ signaling pathways regulate intracellular Ca²⁺ activity in human cardiac fibroblasts. *J. Cell Physiol.* **2010**, *223*, 68–75. [[CrossRef](#)] [[PubMed](#)]
75. Li, M.; Wang, B.; Lin, W. Cl-channel blockers inhibit cell proliferation and arrest the cell cycle of human ovarian cancer cells. *Eur. J. Gynaecol. Oncol.* **2008**, *29*, 267–271.
76. Kim, D.S.; Li, B.; Rhew, K.Y.; Oh, H.W.; Lim, H.D.; Lee, W.; Chae, H.J.; Kim, H.R. The regulatory mechanism of 4-phenylbutyric acid against ER stress-induced autophagy in human gingival fibroblasts. *Arch. Pharm. Res.* **2012**, *35*, 1269–1278. [[CrossRef](#)]